Journal of Alloys and Compounds 513 (2012) 44–49

Contents lists available at SciVerse ScienceDirect

Journal of Alloys and Compounds

journal homepage: www.elsevier.com/locate/jallcom

Effect of thermal treatment on the characteristics of iridium Schottky barrier diodes on n-Ge (1 0 0)

A. Chawanda[a,b,*], S.M.M. Coelho[a], F.D. Auret[a], W. Mtangi[a], C. Nyamhere[c], J.M. Nel[a], M. Diale[a]

[a] *Department of Physics, University of Pretoria, 0002, South Africa*
[b] *Department of Physics, Midlands State University, Bag 9055, Gweru, Zimbabwe*
[c] *Department of Physics, Nelson Mandela Metropolitan University, Box 77000, Port Elizabeth 6031, South Africa*

ARTICLE INFO

Article history:
Received 22 November 2010
Received in revised form
16 September 2011
Accepted 19 September 2011
Available online 6 October 2011

Keywords:
Schottky contact
Germanium
Annealing
Ideality factor
Agglomeration

ABSTRACT

Iridium (Ir) Schottky barrier diodes were deposited on bulk grown (1 0 0) Sb-doped *n*-type germanium by using the electron beam deposition system. Electrical characterization of these contacts using current–voltage (*I–V*) and capacitance–voltage (*C–V*) measurements was performed under various annealing conditions. The variation of the electrical properties of these Schottky diodes can be attributed to combined effects of interfacial reaction and phase transformation during the annealing process. Thermal stability of the Ir/n-Ge (1 0 0) was observed up to annealing temperature of 500 °C. Furthermore, structural characterization of these samples was performed by using a scanning electron microscopy (SEM) at different annealing temperatures. Results have also revealed that the onset temperature for agglomeration in a 20 nm Ir/n-Ge (1 0 0) system occurs between 600 and 700 °C.

© 2011 Elsevier B.V. All rights reserved.

1. Introduction

Schottky barrier diodes (SBDs) have already been studied for more than 50 years and they have been used in many applications such as gates for metal-semiconductor field-effect transistors, solar cells, and detectors [1–4]. Schottky contacts play an important role in controlling the electrical performances of semiconductor devices and Schottky barrier height (SBH) which is highly sensitive to thermal treatment [5]. Microelectronics has primarily been a Si-based technology because of the stability and high quality of SiO_2 [6], as stability and reproducibility of contact properties are essential prerequisites for device development [2,7,8]. As the scaling of silicon complementary metal-oxide semiconductor (CMOS) devices becomes more and more challenging, both innovative structures and new materials with high carrier mobility are needed to continue improving the device performance [9]. Germanium (Ge) has been regarded as a possible replacement for Si as the channel material in future high-speed CMOS technology, because it offers two times higher intrinsic electron mobility and four times higher intrinsic hole mobility than Si [10]. The lack of a stable native Ge oxide has been the obstacle in the use of Ge in CMOS devices [11]. However, recent developments of the next generation deposited high-*k* gate dielectrics allow for the fabrication of high performance Ge-based metal-oxide semiconductor field effect transistors (MOSFETs) [11,12]. Low reactivity with oxygen in the high-*k* dielectric is expected in the germanide/high-k gate stack structure [13].

Although in previous studies focus has been on the reactions of germanium with Pd [6,14–23], Pt [6,13,22,24–29], and Ni [6,9,11,13–16,22,28–38], so far there is very little literature on reactions of germanium with Ir [39]. Gaudet et al. [6] carried out a systematic study of thermally induced reaction of 20 transition metals with Ge substrates. They monitored metal-Ge reactions in situ during ramp anneals at 3 °C s^{-1} using time-resolved X-ray diffraction, diffuse light scattering, and resistance measurements. Their results show that Fe, Co, Ni, Pd, Pt, and Cu were the most promising candidates for microelectronic applications. A reduction of the PtGe/Ge electron SBH by rapid thermal diffusion of phosphorous was reported by Henkel et al. [24]. Their results show that rapid thermal diffusion from a solid diffusion doping source is effective in reducing SBHs of platinum germanide SBDs on Ge. Saedi et al. [25] reported a scanning tunneling microscopy and spectroscopy study of the formation of platinum–germanide phases on Ge (1 1 1). Chawanda et al. [28] investigated the change in the (*I–V*) electrical properties of Pt-, Ni- and Ti Schottky diodes on n-Ge (1 0 0) at different annealing temperatures. Their results reveal that the as-deposited barrier heights have values that are near the bandgap of Ge for Pt/-, Ni/- and Ti/n-Ge (1 0 0) Schottky

* Corresponding author at: Department of Physics, University of Pretoria, 0002, South Africa. Tel.: +27 12 420 3508; fax: +27 12 362 5288.
E-mail address: albert.chawanda@up.ac.za (A. Chawanda).

0925-8388/$ – see front matter © 2011 Elsevier B.V. All rights reserved.
doi:10.1016/j.jallcom.2011.09.053

diodes resulting in good Schottky source/drain contact materials in p-channel Ge-MOSFETS, for the hole injection from source into inverted p-channel [40]. Peng et al. [36] reported on the *I–V* characteristics of Ni/n-Ge (1 0 0) Schottky diodes and the nickel germanide induced strain after subjecting the Schottky contacts to rapid thermal anneal in the temperature range of 300–600 °C. Their results also show that the orthorhombic structure of NiGe induces epitaxial tensile strain on Ge substrate due to the difference in lattice constants. They also suggested that the increase in barrier height with increasing annealing temperature may be due to the conduction band edge shift by the strain after germanidation process. Peng et al. [37] have also reported micro-Raman studies on nickel germanides formed on (1 1 0) crystalline Ge. Their results reveal that Ni_5Ge_3, NiGe and Ni_2Ge phases are formed sequentially with increasing annealing temperatures from 300 °C to 600 °C on n-Ge (1 1 0) substrate. Perrin et al. [38] investigated the phase formation and growth kinetics for both Ni–Si and Ni–Ge systems. They have shown that the Ni–Si system has three major phases (Ni_2Si, NiSi and $NiSi_2$) that grow sequentially while Ni–Ge system showed only two phases (Ni_5Ge and NiGe) that grow simultaneously. Habanyama and Comrie [39] used ion beam analysis employing micro-Rutherford backscattering spectrometry to investigate the interaction between germanium and iridium in a lateral diffusion couple. Their results indicate that the germanide phase Ir_3Ge_7 stretches across the original island interface at all annealing temperatures, with a phase Ir_4Ge_5 forming in the reaction region with unreacted iridium. The phase $IrGe_4$ was observed to nucleate in the middle of the island at annealing temperatures above 800 °C.

In this work we investigate the change in the electrical properties of Ir Schottky barrier diode on n-Ge (1 0 0) at different annealing temperatures in the temperature range 25–500 °C. Results presented here reveal the effects of thermal treatment, particularly the combined effects of interfacial reaction and phase transition [41] of Ir/n-Ge (1 0 0) Schottky barrier diodes using the *I–V* and *C–V* characteristics. Furthermore, morphological evolution of Ir films on n-Ge (1 0 0) is studied using the scanning electron microscopy (SEM) characterization method.

2. Experimental procedures

To study the thermal annealing effects on the Schottky barrier diode, we have used bulk-grown (1 0 0) oriented n-type Ge doped with antimony (Sb) to a density of $(1.5–2.0) \times 10^{15}$ cm^{-3} and supplied by Umicore. Before metallization, the samples were first degreased and subsequently etched in a mixture of H_2O_2 (30%): H_2O (1:5) for 1 min. Immediately after cleaning they were inserted into a vacuum chamber where AuSb (0.6% Sb), 120 nm thick, was deposited by resistive evaporation on their back surfaces as ohmic contacts. The samples were then annealed at 350 °C in Ar ambient for 10 min to minimize the contact resistivity of the ohmic contacts [42]. Before Schottky barrier diodes deposition, the samples were again chemically cleaned as described above. Ir Schottky barrier diodes were deposited onto Ge wafers using electron beam evaporation through a mechanical mask. The contacts were (0.60 ± 0.05) mm in diameter and 20 nm thick. The metal thickness layer and deposition rates were monitored by using an INFICON XTC 751-001-G1 quartz crystal thickness monitor. After Schottky barrier diode fabrication, the samples were characterized by *I–V* measurements at room temperature to determine the quality of the diodes. The Schottky barrier diodes were then isochronally annealed in an oven under Ar ambient in the temperature range 25 °C to 500 °C in steps of 25 °C for 30 min. *I–V* and *C–V* characteristic measurements followed each additive annealing cycle. Characterization of the Ir films at different annealing temperatures was accomplished using a ZEISS ULTRA PLUS Scanning electron microscopy (SEM) system operating at 1 kV.

3. Results and discussion

The Schottky barrier heights of the diodes were deduced from *I–V* characteristics, which were analyzed by using the thermionic emission model [7,43]:

$$I(V) = I_o \quad \exp\left(\frac{qV}{nkT}\right)\left[1 - \exp\left(-\frac{qV}{kT}\right)\right] \tag{1}$$

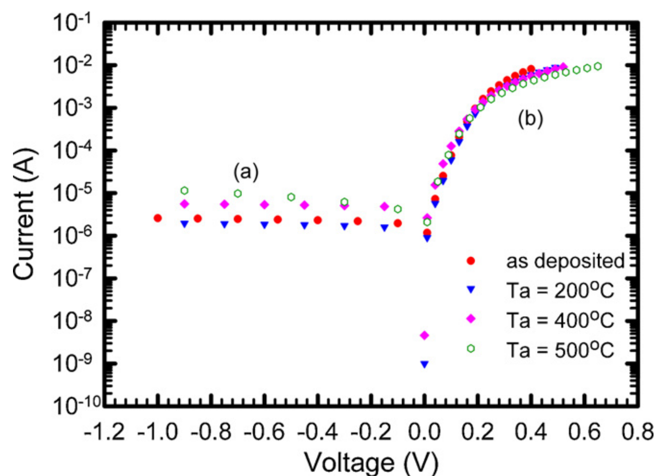

Fig. 1. Experimental (a) reverse and (b) *I–V* characteristics of one of the Ir/n-Ge (1 0 0) Schottky barrier diodes after isochronal thermal treatment for 30 min at different annealing temperatures: as-deposited, 200 °C, 400 °C and 500 °C.

where I_o is the reverse saturation current given by the following relation [44,45]:

$$I_o = AA^*T^2 \quad \exp\left(-\frac{q\Phi_B}{kT}\right), \tag{2}$$

obtained from the straight line intercept of $\ln I$ at $V = 0$, A^* is the effective Richardson constant, A is the diode area, T the measurement temperature, k the Boltzmann constant, Φ_B is the zero bias effective Schottky barrier height (SBH), q is the electronic charge and n the ideality factor which can be determined accurately from the slope of the linear part of a ln I versus V plot, assuming pure thermionic emission can be obtained from Eq. (1) as

$$n = \frac{q}{kT}\frac{dV}{d(\ln(I))} \tag{3}$$

The value on n is equal to 1.0 for an ideal diode and usually has a value greater than unit.

We fabricated eight Ir/n-Ge (1 0 0) Schottky barrier diodes (SBDs). Fig. 1 shows the semilog forward and reverse bias *I–V* characteristics of these SBDs for as-deposited samples and after annealing the samples in the temperature range of 25–525 °C. Since the annealing temperature range is wide, we have assumed that the change in thermal properties of Ir/n-Ge (1 0 0) SBDs (e.g. thermal expansion) have negligible effects on our results. Using Eq. (2) and intercept of the straight line fit of the semilog-forward bias *I–V* graph the value of effective SBH is determined.

Fig. 2 presents the variation of the Schottky barrier height and reverse current at −1 V with annealing temperature for the Ir Schottky diodes. The SBH and reverse current at a bias voltage of −1 V for as-deposited Ir Schottky diodes were found to be (0.574 ± 0.005) eV and (2.57 ± 0.02) μA, respectively. After annealing at temperatures higher than 200 °C, the Schottky barrier height (SBH) drops significantly, reaching (0.542 ± 0.005) eV after a 400 °C anneal. We suggest that there is a significant reaction between Ir and Ge. The change coincides with the initial phase formation of the germanides IrGe and Ir_4Ge_5, which have been reported by Habanyama and Comrie [39] to coexist and form at annealing temperatures around 350 °C. Bhan and Schubert [46] also reported the phases IrGe and Ir_4Ge_5 to coexist in bulk diffusion couples. The change in the barrier height after the 400 °C anneal coincides with the temperature of formation of Iridium germanide Ir_3Ge_7, reported by Habanyama and Comrie [39] to form after 400 °C anneal. Fig. 2 also depicts that, throughout the annealing process the reverse current at −1 V remains in the same order of magnitude, 10^{-6} A. Annealing at temperatures higher than 500 °C resulted in near ohmic contacts and

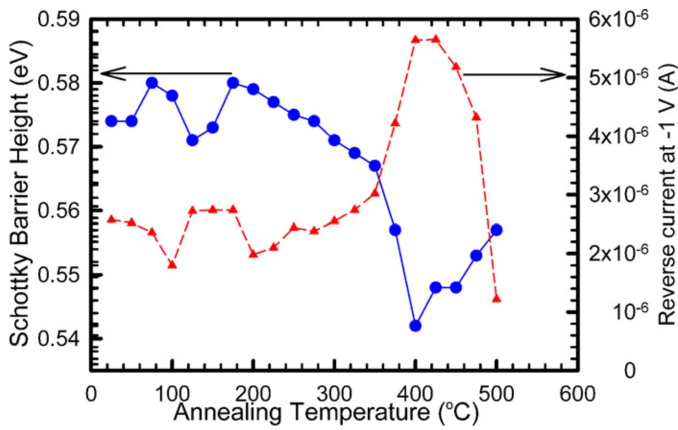

Fig. 2. Plot of the Schottky barrier height and reverse current at −1 V as a function of annealing temperature for Ir/n-Ge (1 0 0) Schottky barrier diode.

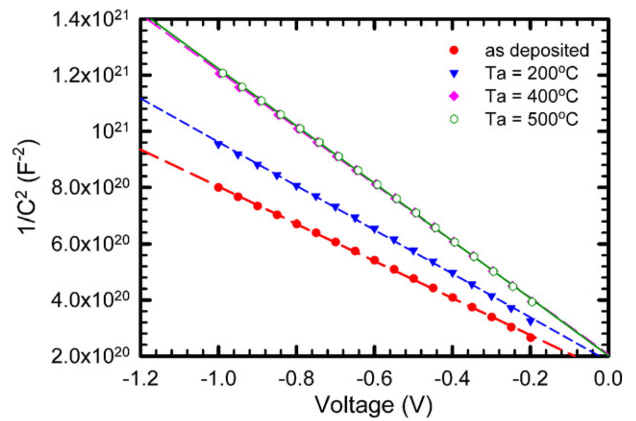

Fig. 5. Reverse bias C^{-2}–V characteristics of one of the Ir/n-Ge (1 0 0) Schottky barrier diodes frequency of 1 MHz after isochronal treatment for 30 min at different annealing temperatures: as-deposited, 200 °C, 400 °C and 500 °C.

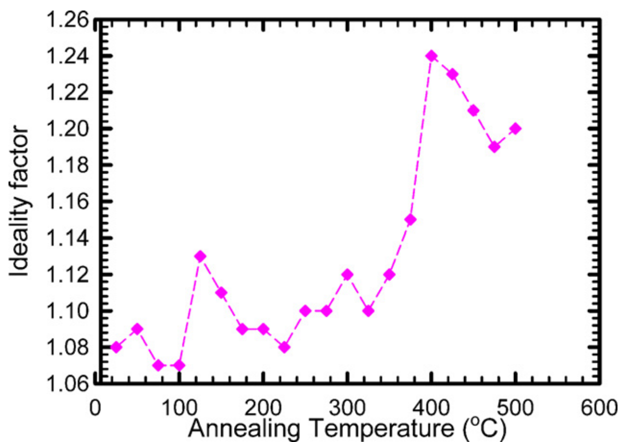

Fig. 3. Plot of ideality factor as a function of annealing temperature for Ir/n-Ge (1 0 0) Schottky barrier diode

further analysis of the I–V and C–V characteristics of the Ir Schottky barrier diodes was not possible. These results show that Ir/n-Ge (1 0 0) Schottky diodes are thermally stable over a wide range of temperature, 25–500 °C. Similar results have been reported by [6,23,28]. Pd/n-Ge Schottky diodes have been observed to be stable over a wide temperature range 25–525 °C [6,23]. Pt/n-Ge Schottky diodes have been reported to be thermally stable in the temperature range of 25–600 °C [28].

The SBH is likely to be a function of the interface atomic structure, and atomic inhomogeneities at MS interface which are caused by grain boundaries, multiple phases, facets, defects, a mixture of different phases, etc. [47,48]. It is well known that the chemical reactions between metals and semiconductors at interfaces can play an important role in the electrical properties of devices. Boyarby et al. [49] suggested that the recent motivation for studying Schottky barrier formation is due to the recognition that both electronic and chemical equilibrium have to be considered together across a reactive interface between metal and semiconductor, as surface states and metal-induced gap states failed to take into consideration the chemical equilibrium at interface. The chemical equilibrium after a heat treatment results in interfacial atomic rearrangement, interdiffusion, and compound formation, which should have a profound effect on the electronic equilibrium producing the Schottky barrier [50]. Hence, the change in Schottky barrier heights may be attributed to combined effects of interfacial reaction and phase transformation [51].

The ideality factor was calculated from the gradient of the linear region of the experimental $\ln I$–V characteristics in forward bias [7]. The variation of the Ir Schottky diodes ideality factor as a function of annealing temperature is shown in Fig. 3. The as-deposited value of the ideality factor was found to be 1.08. At annealing temperatures between 275 and 500 °C, ideality factors significantly greater than 1.1 indicate that the transport properties are not well modeled by thermionic emission alone although their contacts remain rectifying [52]. The non-idealities are mostly

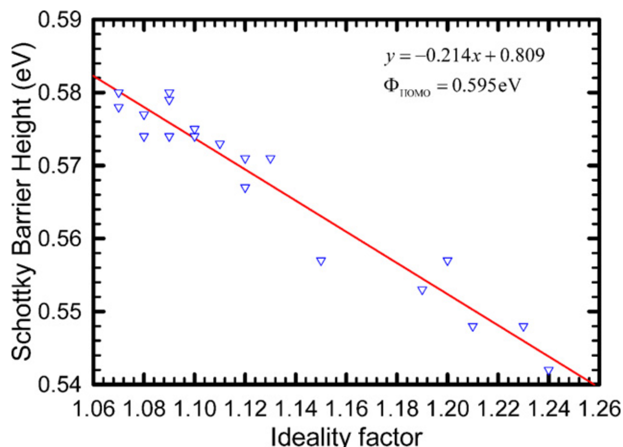

Fig. 4. The plot of Schottky barrier heights as a function of their respective ideality factors of Ir/n-Ge (1 0 0) Schottky barrier diode at various annealing temperatures.

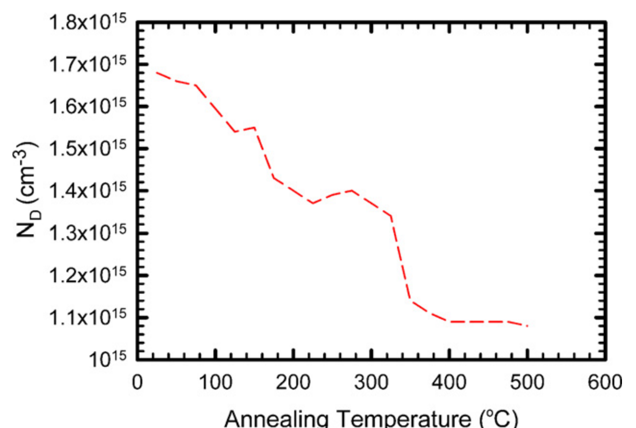

Fig. 6. The variation of non-compensated ionized donors (N_D) concentration with annealing temperature.

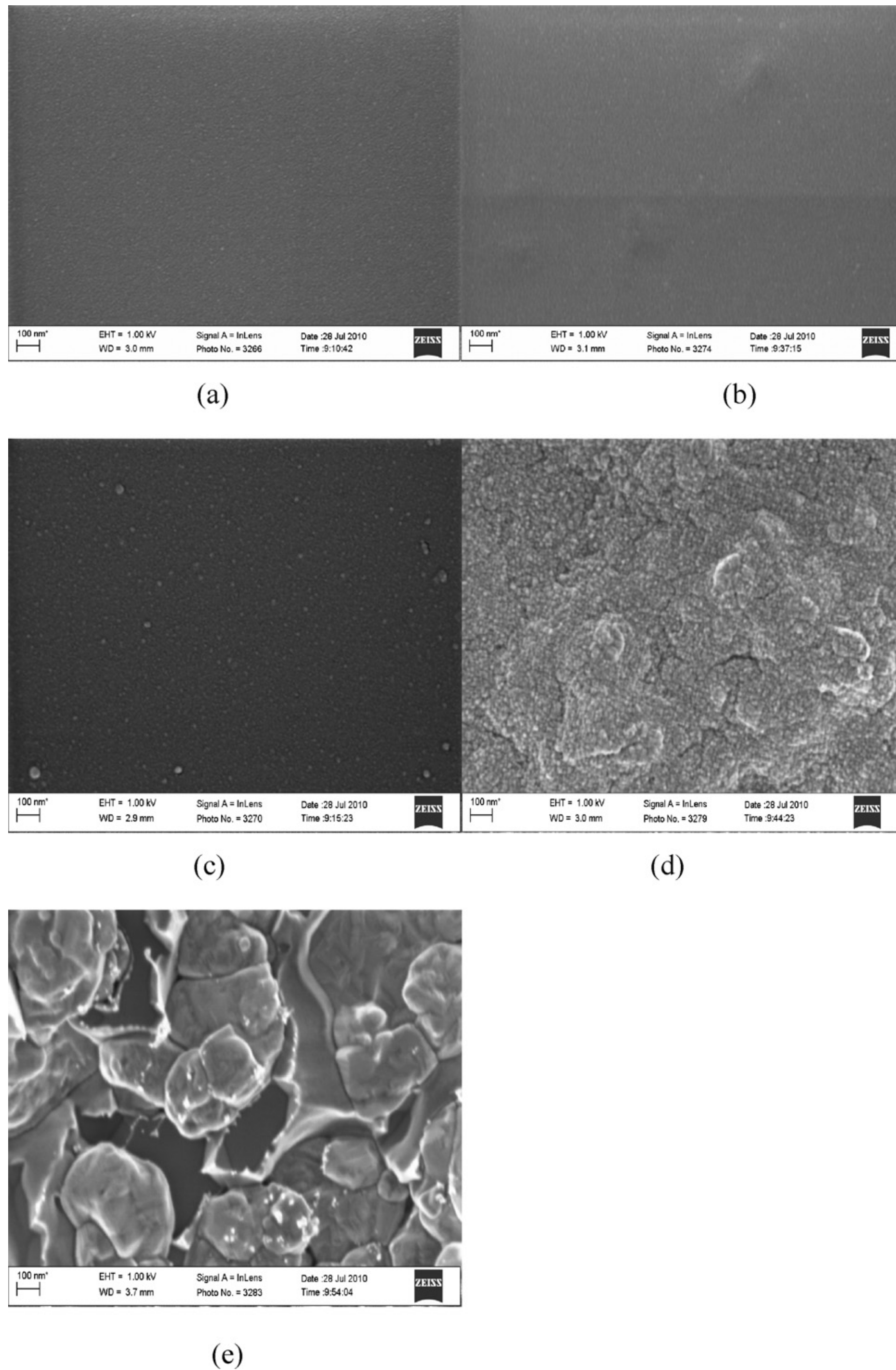

Fig. 7. SEM observations for Ir films on germanium after isochronal thermal treatment for 30 min at different annealing temperatures: (a) as-deposited, (b) 400 °C, (c) 500 °C, (d) 600 °C and (e) 700 °C.

due to the states associated with the defects near the surface of the semiconductor [7]. In a Schottky contact, even with a good surface treatment, there is an interfacial oxide layer of thickness about 1 nm with considerable amount of surface states [7]. These interface states, and inter-diffusion, chemical reaction, compound formation, defects generation, etc. can all be derived from thermodynamics due to thermal annealing [8,53,54]. These may result in the formation of recombination centres [52] and SBH inhomogeneities [55], which cause an excess current leading to a deviation from the ideal thermionic emission behaviour. Additionally, there are other sources of SBH inhomogeneity. For instance, there may be a mixture of different metallic phases with different SBHs due to incomplete interfacial reaction, and doping inhomogeneity at a MS interface [56]. Thus, the current across the MS contact may be mainly due to the presence of SBH inhomogeneity and this inhomogeneity leads to large ideality factors.

Fig. 4 shows a plot of the SBHs as a function of their respective ideality factors, obtained from the annealing process in the temperature range 25–500 °C. The straight line in Fig. 4 is the least-squares fit to experimental data. Since the results show a linear correlation between SBHs and ideality factors, we extrapolated the plot to $n = 1.0$, and obtained a laterally homogeneous SBH of 0.595 eV

for Ir/n-Ge (1 0 0) Schottky barrier diodes. The homogeneous SBHs rather than effective SBHs of Schottky diodes or their mean values should be used to discuss theories on the physical mechanisms that determine the SBHs of MS contacts [57,58].

Fig. 5 shows the plots of Ir/n-Ge (1 0 0) Schottky barrier diodes reverse bias C^{-2}–V characteristics at 1.0 MHz at different annealing temperatures. The plots of C^{-2} as a function of reverse bias voltage are linear, indicating the formation of Schottky diodes [59], and a constant non-compensated ionized donor concentration. In Schottky diodes, the depletion layer capacitance (C), can be expressed as [2,7]:

$$\frac{1}{C^2} = \frac{2(V_0 - V)}{q\varepsilon_s A^2 N_D} \quad (4)$$

where A is the area of the diode, ε_s is the permittivity of semiconductor, N_D is the concentration of non-compensated ionized donors, that can be temperature dependent, V is the magnitude of the reverse bias and V_0 is the diffusion potential at zero bias. From Eq. (4), the values of V_0 and N_D can be determined from the intercept and slope of the C^{-2}–V plot. The C–V SBH for as-deposited Ir/n-Ge (1 0 0) Schottky barrier diode was found to be (0.473 ± 0.005) eV. Due to the different nature of the measurement techniques, SBHs obtained from I–V and C^{-2}–V are not always the same [60]. Although, in general, SBHs from C–V measurements are higher than SBHs from I–V measurements, in our study, we obtained I–V SBHs that were higher than C–V SBHs. Similar results have been reported [35]. Therefore, further studies are needed to clarify these results. Fig. 6 depicts the variation of non-compensated ionized donor concentration with annealing temperature. The non-compensated ionized donor concentration decreases with annealing temperature. Similar results have been reported by Serin [61], Nuhoglu and Gulen [62] and Opsomer et al. [63]. This may be due to either presence of high density of compensating deep acceptor levels [61], possibly related to in-diffused Ir or the decrease in the dangling bonds due to annealing [62] and formation of Iridium germanide [39].

SEM observations were conducted for Ir/n-Ge (1 0 0) samples, as-deposited and after annealing at different temperatures. The morphological evolution is shown in Fig. 7. As seen in Fig. 7(a) and (b), metal surfaces show little change when samples were annealed below 400 °C. Grain growth at the surface (see Fig. 7(c)) were evident after a 500 °C anneal, indicating inception of agglomeration. Agglomeration starts with grain boundary grooving and progresses to island formation [64]. We observed development of severe grain grooving after a 600 °C anneal (see Fig. 7(d)). We also observed that after 700 °C anneal (see Fig. 7(e)), film continuity was severely interrupted as revealed by dark spots caused by exposed Ge regions. From these observations we conclude that the onset of the agglomeration process for 20 nm Ir/n-Ge (1 0 0) system occurs between 600 and 700 °C. The morphological degradation for Ni–Ge, Pd–Ge and Pt–Ge begins at 580, 550, and 600 °C, respectively [6,28]. We suggest a good morphological stability for Ir germanide films up to 500 °C.

4. Conclusions

Ir Schottky barrier diodes were fabricated by using an electron beam deposition system. The Schottky barrier diodes behaviour was investigated under various annealing conditions. The variation of Schottky barrier heights and ideality factors with annealing may be attributed to interfacial reactions of Ir with germanium and phase transformation of Ir germanides during the annealing process. The electrical properties reveal that Ir Schottky barrier diodes are of high quality with low reverse currents at −1 V of the order 10^{-6} A and as-deposited ideality factors as low as 1.08. The homogeneous SBH value of 0.595 eV for the Schottky barrier diodes was obtained from the linear relationship between SBHs and their respective ideality factors. The homogeneous SBH near the bandgap of Ge in Ir/n-Ge (1 0 0) Schottky barrier diodes imply good Schottky source/drain contact material in p-channel Ge-MOSFETS, for the hole injection from source into inverted p-channel [40]. Thermal stability of the Ir/n-Ge (1 0 0) Schottky barrier diodes is maintained up to annealing temperature of 500 °C. Furthermore, SEM observations were conducted for samples annealed at different temperatures, and the results depict that the onset temperature for agglomeration in 20 nm Ir/n-Ge (1 0 0) system occurs between 600 and 700 °C. From these results we conclude that Ir is a promising candidate for its use as first level interconnections in Ge-based microelectronic circuits.

Acknowledgements

This work has been made possible by financial assistance from the South African National Research Foundation. The authors gratefully acknowledge SEM observation measurements by Helena Steyn.

References

[1] E. Hökelek, G.Y. Robinson, Solid State Electron. 99 (1981) 24.
[2] E.H. Rhoderick, R.H. Williams, Metal-semiconductor Contacts, Clarendon Press, Oxford, 1988.
[3] G.A. Barti, M. Schlilter, Phys. Rev. B 33 (1986) 7346.
[4] A. Asubay, Ö. Güllü, A. Türüt, Appl. Surf. Sci. 254 (2008) 3558.
[5] A.R. Saha, S. Chattopadhyay, C.K. Maiti, Mater. Sci. Eng. B 114–115 (2004) 218.
[6] S. Gaudet, C. Detavernier, A.J. Kellock, P. Desjardins, C. Lavoie, J. Vac. Sci. Technol. A 24 (2006) 474.
[7] S.M. Sze, Physics of Semiconductor Devices, 2nd ed., Wiley, New York, 1981.
[8] T. Sands, Appl. Phys. Lett. 52 (1988) 197.
[9] H. De-Dong, L. Xiao-Yan, K. Jin-Feng, X. Zhi-Liang, D. Gang, H. Ru-Qi, Chin. Phys. 14 (2005) 1041.
[10] R. Li, H.B. Yao, S.J. Lee, D.Z. Chi, M.B. Yu, G.Q. Lo, D.L. Kwong, Thin Solid Films 504 (2006) 28.
[11] D.Z. Chi, H.B. Yao, S.L. Liew, C.C. Tan, C.T. Chua, K.C. Chua, R. Li, S.J. Lee, 7th International Workshop on Junction Technology Proceeding, 2007.
[12] C.O. Chui, S. Ramanathan, B.B. Triplett, P.C. McIntyre, K.C. Saraswat, IEEE Electron Dev. Lett. 23 (2002) 473.
[13] D. Ikeno, Y. Kaneko, H. Kondo, M. Sakashita, A. Sakai, M. Ogawa, S. Zaima, Jpn. J. Appl. Phys. 46 (2007) 1865.
[14] A. Thanailakis, D.C. Northrop, Solid State Electron. 16 (1973) 1383.
[15] M. Wittmer, M.-A. Nicolet, J.W. Mayer, Thin Solid Films 42 (1977) 51.
[16] I. Abbati, G. Rossi, L. Braicovich, I. Lindau, W.E. Spicer, Appl. Surf. Sci. 9 (1981) 243.
[17] G. Majni, G. Ferrari, C. Canali, F. Catellani, G. Ottaviani, G. Della Mea, Thin Solid Films 47 (1977) 193.
[18] G. Ottaviani, G. Majni, G. Ferrari, R. Ferrari, M. Prudenziati, S.S. Lau, Thin Solid Films 47 (1977) 187.
[19] G. Ottaviani, G. Majni, C. Canali, Appl. Phys. 18 (1979) 285.
[20] Y.F. Hsieh, L.J. Chen, Thin Solid Films 162 (1988) 295.
[21] C.L. Churms, C.M. Corie, R.S. Nemtudi, Nucl. Instr. Methods B 158 (1999) 713.
[22] E. Simoen, K. Opsomer, C. Claeys, K. Maex, C. Detavernier, R.L. Van Meirhaeghe, P. Clauws, J. Electrochem. Soc. 154 (2007) H857.
[23] A. Chawanda, C. Nyamhere, F.D. Auret, W. Mtangi, T.T. Hlatshwayo, M. Diale, J. Nel, Physica B 404 (2009) 4482.
[24] C. Henkel, S. Abermann, O. Bethege, G. Pozzovivo, S. Puchner, H. Hutter, E. Bertagnolli, J. Electrochem. Soc. 157 (2010) H815.
[25] A. Saedi, B. Poelsema, H.J.W. Zandvliet, Surf. Sci. 605 (2011) 507.
[26] V. Janardhanam, J.-S. Kim, K.-W. Moon, K.-S. Ahn, C.-J. Choi, Microelectron. Eng. (2011), doi:10.1016/j.meee.2011.04010.
[27] R.S. Nemutudi, C.M. Comrie, C.L. Churns, Thin Solid Films 358 (2000) 270.
[28] A. Chawanda, C. Nyamhere, F.D. Auret, W. Mtangi, M. Diale, J.M. Nel, J. Alloys Compd. 492 (2009) 649.
[29] C. Nyamhere, A. Chawanda, A.G.M. Das, F.D. Auret, M. Hayes, Physica B 401–402 (2007) 226.
[30] T. Nishimura, O. Nakatsuka, Y. Shimura, S. Takeuchi, B. Vincent, A. Vantome, J. Dekoster, M. Caymax, R. Loo, S. Zaima, Solid-State Electron. 60 (2011) 46.
[31] H.-X. Liu, X.-F. Wu, S.-G. Hu, L.-C. Shi, Chin. Phys. B 19 (2010) 057303.
[32] J.K. Patterson, B.J. Park, K. Ritly, H.Z. Xiao, L.H. Allen, A. Rockett, Thin Solid Films 253 (1994) 456.
[33] K.Y. Lee, S.L. Liew, S.J. Chua, D.Z. Chi, H.P. Sun, X.Q. Pan, Mater. Res. Soc. Symp. Proc. 810 (2004), C.2.4.1.
[34] D. Han, Y. Wang, D. Tian, W. Wang, X. Liu, J. Kang, R. Han, Microelectron. Eng. 82 (2005) 93.
[35] A. Chawanda, J. Nel, F.D. Auret, W. Mtangi, C. Nyamhere, M. Diale, L. Leach, J. Kor. Phys. Soc. 57 (2010) 1970.

[36] C.-Y. Peng, Y.-H. Yang, C.-M. Lin, Y.-J. Yang, C.-F. Huang, C.W. Liuv, International Conference on Solid-state and Integrated Circuits Technology Proceedings (ICSICT), 2008, p. 681, art. no. 4734645.
[37] C.-Y. Peng, C.-F. Huang, Y.-H. Yang, C.W. Liu, ECS Trans. 16 (2008) 249.
[38] C. Perrin, D. Mangelinck, F. Nemouchi, J. Labar, C. Lavoie, C. Bergman, P. Gas, Mater. Sci. Eng. B 154–155 (2008) 163.
[39] A. Habanyama, C.M. Comrie, Thin Solid Films 516 (2008) 5137.
[40] H.B. Yao, C.C. Tan, S.L. Liew, C.T. Chua, C.K. Chua, R. Li, R.T.P. Lee, S.J. Lee, D.Z. Chi, International Workshop on Junction Technology Proceeding, 2006, p. 64.
[41] Y. Sun, X.M. Shen, J. Wang, D.G. Zhao, G. Feng, Y. Fu, Y. Fu, S.M. Zhang, Z.H. Zhang, Z.H. Feng, Y.X. Bai, H. Yang, J. Phys. D: Appl. Phys. 35 (2002) 2648.
[42] F.D. Auret, P.J. Janse van Rensburg, M. Hayes, J.M. Nel, S. Coelho, W.E. Meyer, S. Decoster, V. Matias, A. Vantomme, D. Smeets, Nucl. Instr. Methods B 257 (2007) 169.
[43] I.S. Yahia, M. Fadel, G.B. Sark, F. Yakuphanoglu, S.S. Shenouda, W.A. Farooq, J. Alloys Compd. 509 (2011) 4414.
[44] H. Uslu, S. Altindal, U. Aydemir, I. Dokme, I.M. Afandiyeva, J. Alloys Compd. 503 (2010) 96.
[45] F. Yakuphanoglu, J. Alloys Compd. 494 (2010) 451.
[46] S. Bhan, K. Schubert, Z. Metallkd. 51 (1960) 327.
[47] J.P. Sullivan, R.T. Tung, M.R. Pinto, W.R. Graham, J. Appl. Phys. 70 (1991) 7403.
[48] R.T. Tung, Mater. Sci. Eng. Rep. 35 (2001) 1.
[49] B. Boyarby, H. Çetin, M. Kaya, E. Ayyildiz, Microelectron. Eng. 85 (2008) 721.
[50] R.D. Thomson, K.N. Tu, J. Appl. Phys. 53 (1982) 4285.
[51] Y. Sun, X.M. Shen, J. Wang, D.G. Zhao, G. Feng, Y. Fu, S.M. Zhang, Z.H. Zhang, Z.H. Feng, Y.X. Bai, H. Yang, J. Phys. D: Appl. Phys. 35 (2002) 2648.
[52] H. Doğan, N. Yildirim, A. Turut, Microelectron. Eng. 85 (2008) 655.
[53] S.K. Cheung, N.W. Cheung, Appl. Phys. Lett. 49 (1986) 85.
[54] J.L. Everaet, R.L. Van Meirhaeghe, W.H. Laflere, F. Cardon, Semicond. Sci.Technol. 5 (1990) 60.
[55] R.T. Tung, J.P. Sullivan, F. Schrey, Mater. Sci. Eng. B 14 (1992) 266.
[56] M. Soylu, F. Yakuphanoglu, J. Alloys Compd. 506 (2010) 418.
[57] R.F. Schmitsdorf, T.U. Kampen, W. Mönch, J. Vac. Sci. Technol. B 15 (1997) 1221.
[58] H. Çetin, B. Şahin, E. Ayyilidiz, A. Turut, Semicon. Sci. Technol. 19 (2004) 1113.
[59] V. Saxen, R. Prakash, Polym. Bull. 45 (2000) 267.
[60] G. Güler, Ş. Karataş, Ö. Güllü, Ö.F. Bakkaloğlu, J. Alloys Compd. 486 (2009) 343.
[61] T. Serin, Turk. J. Phys. 22 (1998) 423.
[62] C. Nuhoglu, Y. Gulen, Vacuum 84 (2010) 812.
[63] K. Opsomer, E. Simoen, C. Clayes, K. Maex, C. Detaernier, R.L. Van Meirhaeghe, S. Forment, P. Clauws, Mater. Sci. Semicond. Process. 9 (2006).
[64] K.Y. Lee, S.L. Liew, S.J. Chua, D.Z. Chi, H.P. Sun, X.Q. Pan, Mater. Res. Symp. 810 (2004) 55.